Submonolayer sodium coverages on the surface of the gold film

© *P.A. Dementev*[1], *E.V. Dementeva*[1], *M.N. Lapushkin*[1], *S.N. Timoshnev*[1,2]

[1] Ioffe Institute,
St. Petersburg, Russia
[2] Alferov University,
St. Petersburg, Russia

E-mail: Lapushkin@ms.ioffe.ru

Photoelectron spectroscopy studies of the electronic structure of a 2D-Au film deposited on a W surface with a natural oxide have been carried out *in situ* in ultrahigh vacuum, before and after adsorption of Na atoms. The photoemession spectra from the valence band and core levels of Au $4f$, W $4f$ and Na $2p$ were studied under synchrotron excitation in the photon energy range of $120-300$ eV. A 0.83 nm thick 2D gold film formed on the tungsten surface has a valence band close to the valence band of the bulk sample. The diffusion of Na atoms deep into the gold film was not detected, which indicates the layer-by-layer growth of the 2D-Au film. Two states have been found: $Na^{\delta+}$ and Na^+, which exist even with a 0.15 monolayer sodium coverage, that indicates the formation of Na islands and single adsorption of Na atoms. The density functional method is used to calculate the electronic structure of a 2D-Au layer without and with adsorbed Na. It is established that the adsorption of Na atoms in the hollow or bridge position is preferable. It is found that the Na adsorption leads to the surface reconstruction.

Keywords: adsorption, sodium, gold, surface reconstruction, photoemission, density functional method.

1. Introduction

Research on the adsorption of particles on the surface of solids has been carried out for many decades and tens of thousands of works have been devoted to it. The alkali metal atom adsorption on a metal substrate may be assumed as a model system due to its apparent simplicity. It would seem that everything has been already studied and various processes taking place on these surfaces have been investigated. For many adsorption systems, the nature of the chemical bond, the geometrical and electronic surface structure, the work function, the binding energies of adatoms, etc., are known.

Several investigations were focused on the sodium adsorption on gold surface both on the bulk sample surface and on the 2D gold film surface. In [1], sodium adsorption on the (5×20) reconstructed Au(100) surface was investigated and it was reported that even deposition of a 0.4 monolayer (ML) of sodium results in transformation of the surface with (1×2) structure. It is also shown that Na $1s$ level shift by 0.8 eV takes place with increase sodium coverage from 0.16 to 1.3 ML. It should be noted that the reported work function achieved the plateau at 0.5 ML coating. In [2], the sodium adsorption on Au(111) surface was studied by the scanning tunneling microscopy method. It is shown that poorly ordered hexagonal structure is formed at 0.46 ML sodium coating that is associated with weakening of the bond between the first and second gold layers due to the interaction between the sodium adatoms and gold surface atoms. In [3], sodium adsorption on

Au(111) was studied in a wide temperature range. It is shown that the sodium atom (coating) adsorption at room temperature leads to surface reconstruction. Deposition of 0.46 ML sodium causes the transformation of the Au(111) chevron surface structure into a poorly ordered domain structure with an isotropically compressed surface layer and hexagonal symmetry. Deposition of more than one sodium monolayer results in formation of $NaAu_2$ intermetallic compound. In [4], the adsorption of sodium atoms (0.05 ML) on gold nanoparticles deposited on tungsten was studied. Deposition of such amount of sodium on the gold nanoparticles does not lead to any perceptible changes in the valence band spectrum, however, the system heating causes perceptible changes in the valence band spectrum and nanoparticle fusion with increasing of total system surface.

The sodium atom adsorption on the surface of the deposited 2D gold film on tungsten was studied in [5,6]. It is shown that several gold monolayers are formed, when gold is deposited on tungsten [6], and then gold crystallites start growing. The sodium atom adsorption on the surface of the deposited 2D gold film on the oxidized tungsten was studied in [7]. It is suggested that the film is formed according to the Vollmer–Weber mechanism, when gold is deposited on the oxidized tungsten.

Deposition of more than one sodium atom monolayer on the gold surface results in formation of surface $Na_x Au_y$ intermetallic compound, e.g. [3], and was not addressed herein. The sodium deposition on the gold surface heated to $T = 1000$ K also results in formation of surface $Na_x Au_y$ intermetallic compounds [8]. Note that the sodium

adsorption in the submonolayer range on the 2D gold film deposited on the tungsten surface at $T = 300$ K does not result in formation of gold intermetallic compounds [9].

The our study of the initial adsorption stages of sodium atoms on the surface of 2D gold film deposited on the tungsten surface in the presence of a natural oxide layer is described herein and the binding energy of the adsorbed sodium atom on the 2D gold film is calculated.

2. Experimental setup

The photoemission studies were carried out at the Russian-German laboratory at the HZB BESSY II (Berlin, Germany) synchrotron by the photoelectron spectroscopy method with excitation within the photon energy range of $120-300$ eV. Photoelectrons normal to the surface were recorded, the exciting beam was incident on the sample surface at $45°$. Studies of the gold film deposited on the tungsten surface coated with natural oxide before and after sodium deposition were carried out *in situ* in vacuum $P < 5 \cdot 10^{-10}$ Torr at room temperature. The photoemission spectra of the valence band (VB) regiond and the spectra of the Au $4f$, W $4f$ and Na $2p$ core levels were recorded. Full energy resolution was 50 meV. The spectra were reduced to the energy relative to the Fermi E_F level whose position was determined by the low-energy rolloff of the photoelectronic spectrum of the tungsten substrate. For all spectra described below, the background was subtracted by the Shirley method. The atomically clean Na was deposited onto a clean surface of the sample from a standard source. Note that one Na monolayer is taken as a concentration of $1.0 \cdot 10^{15}$ atom/cm^2 at which a densely-packed Na atom layer is formed. Gold and sodium atom coverage was determined, respectively, by the attenuation of the W $4f$ and Au $4f$ core peaks (at the photoemission excitation energy of $h\nu = 120$ eV) by the known inelastic mean free path [10,11]. A probing depth depends on the kinetic energy of photoelectrons: the more the kinetic energy of photoelectrons, the more the photoelectron escape depth. It should be noted that the main contribution to the photoemission at $h\nu = 100-120$ eV is made by photoelectrons from the near-surface region, contribution to the photoelectron photoemission from the sample depth increases with the rise in excitation energy compared with the photoelectrons emitted from the sample surface.

3. Calculation details

Calculations were carried out in QUANTUM ESPRESSO package [12] using the exchange-correlation functional taking into account generalized gradient approximations (GGA) [13] in the form of the Perdew-Burke-Ernzerhof [14]. The influence of ion cores was considered through a norm-conserving pseudopotential [15]. Supercells (100) $2 \times 2 \times 2$ were prepared using open-source GUI program BURAI-1.3 [16]. The kinetic energy cut-off and charge
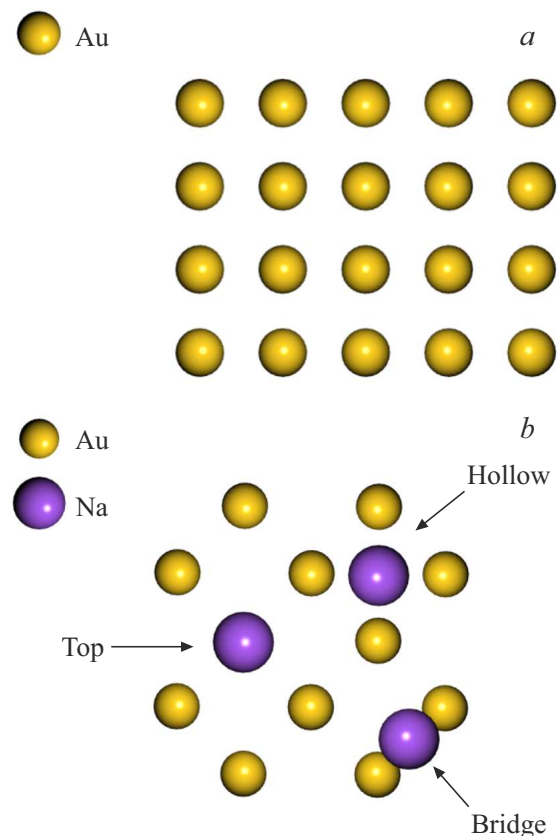
Figure 1. 2D-Au layer (*a*). Na adatom position on 2D-Au layer: top view (*b*). Au atoms are yellow, Na atoms are purple.

density cut-off were set to 55 Ry and 550 Ry. Gamma-centered grid by k-points $4 \times 4 \times 1$ was used for all 2D layers herein. The convergence was equal to $1 \cdot 10^{-6}$ Ry. Geometry optimization was carried out by relaxation of all atom positions in the supercell, except the outer gold atom layer until a pressure lower than 0.5 kbar and force applied to each atom lower than 0.01 eV/Å are achieved. The vacuum gap was set to 18 Å to avoid collapse of 2D layers relative to each other and to ensure geometrical relaxation.

Au has a cubic structure with a lattice constant of 4.17 Å. The supercell contains four Au layers (Figure 1, *a*). The adsorption sites of sodium atoms are shown in Figure 1, *b*: above the Au atom (top), between the Au atoms (bridge) and in the hollow between four neighboring surface Au atoms (hollow). One Na atom account for 8 surface gold atoms.

4. Results and discussion

4.1. Electronic structure

The results of calculating the electronic structure before and after Na atom adsorption are shown in Figure 2. The VB of Au(100) 2D layer is mainly formed by Au $5d$- and $6s$-electrons and coincides with the results, for
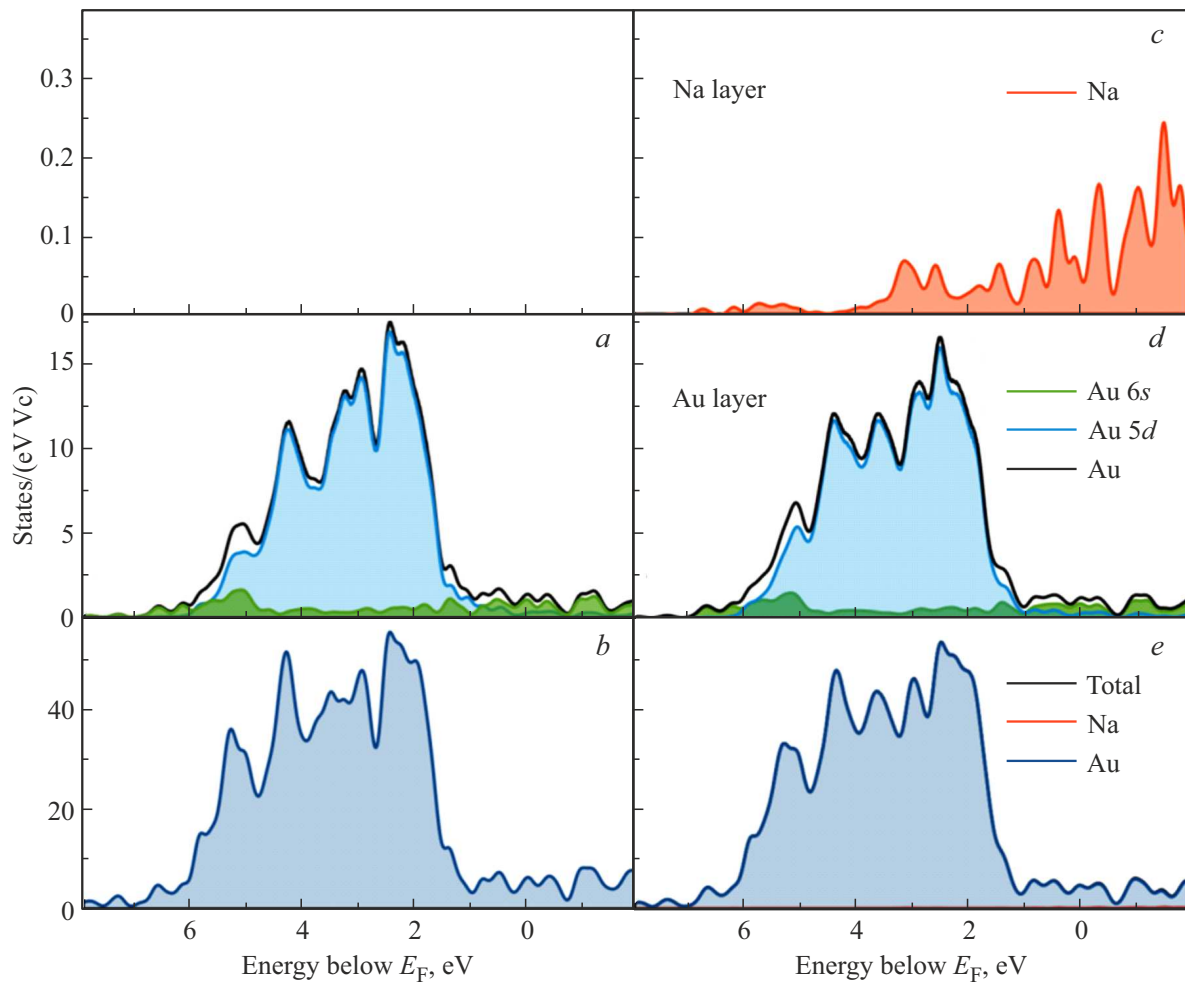
Figure 2. Calculated total (b, e) and partial (a, c, d) density of states in the Na/Au(100) system. The Fermi level is set of 0 eV. Orbital densities of states of Au $6s$ are green, of Au $5d$ are blue and of Au are black. Orbital densities of states of Na $3s$ are red. Density of states of the Au surface layer (a, d). Calculated total and partial density of states for the Au(100) layer (a, b) and after Na adsorption in the hollow position $(c-e)$.

example, [17]. The VB of 2D gold layer after Na atom adsorption is mainly formed by Au $5d$- and $6s$-electrons with a minor admixture of Na $3s$-electrons. The Na atom adsorption does not result in considerable VB spectrum changes that is associated with the interaction of the VB of gold and adsorbed sodium. There are almost no considerable changes in the VB spectrum. For example, maximum density of electron states (DOS) is shifted in the gold surface layer with the binding energy of 2.47 eV for clean gold surface towards higher binding energies by 0.05 eV. Calculations in [18] show that the Na atom adsorption on Au(111) results in minor variation of the VB spectrum shape that is shifted towards lower binding energies by 0.15 eV. The Figure 2 also shows the density of electron states in the gold and sodium surface layer. The Na states band is formed by Na $3s$-electrons.

The adsorption energy of Na adatoms (E_{ads}) was calculated in three positions: on top above the Au (top), between the Au atoms (bridge) and in the hollow between four

Table 1. Na atom adsorption energy and distance between the Au surface layer and adsorbed atom

	E_{ads}, eV	h, Å
hollow	2.85	2.05
top	2.63	2.08
bridge	2.84	1.93

neighboring Au surface atoms (hollow) using the following equation:

$$E_{ads} = -(E_{Au\_Na} - E_{Au} - E_{Na}), \qquad (1)$$

where E_{Au_Na} and E_{Au} are full surface energies with and without adsorbed Na, E_{Na} is the full Na atom energy. The Na atom adsorption energies and distances between the plane formed by the gold surface atom centers and adsorbed Na atom position are given in Table 1.

A similar value $E_{ads} = 2.36\,\text{eV}$ was obtained in the experiment on Na/Ag(111) adsorption system [19]. A high Na adsorption energy equal to 2.7 eV was also achieved in the calculation of the Na/GeP$_3$ system [20].

The Table 1 shows that the adsorption in the hollow position or between Au atoms (bridge) is most preferable, which is followed by the surface layer reconstruction: surface atom shift in the surface plane up to 0.3 Å. These shifts confirm the surface layer reconstruction found earlier in the experiments [1–3]. The distance from the adsorbed Na atom in the hollow position to the Au surface layer is equal to 2.05 Å.

4.2. Gold film

The gold film thickness on tungsten was 0.83 nm. The VB spectra of the deposited gold film on tungsten at the photoemission excitation energy $h\nu = 120\,\text{eV}$ are shown in Figure 3. The spectrum coincides with already known gold VB spectra, e.g. [21,22] and there are two clearly resolved peaks at the binding energies $E_b = 3.7$ and $6.2\,\text{eV}$, which is associated with the excitation of Au $5d$-states.

Figure 4 shows typical spectra of the Au $4f$ core level at the excitation energies $h\nu = 140$ and $300\,\text{eV}$. A slight asymmetry of the peak shape towards lower binding energies is shown and is typical for metals and may be attributable, for example, to the electron excitation to the unoccupied state continuum [23]. However, there is currently no consensus regarding the nature of this effect [24–27]. The spectrum shape is properly described by the Doniach–Sunjic function.

As shown above, there is a natural tungsten oxide consisting of W^{6+} and W^{4+} oxides on the tungsten surface. Gold deposition does not lead to reactions between the gold and tungsten atoms, which leads to the synchronous decrease of W^{6+} and W^{4+} and W^{0} peaks. The W $4f$ doublet core level spectrum of the tungsten oxides and metallic tungsten for the clean oxidized tungsten surface at the excitation energy $120\,\text{eV}$ is shown in Figure 5, a. The same Figure shows decomposition of the experimental spectrum into components described by the Gaussian function. A narrow peak corresponding to the excitation of W^0 $4f_{5/2}$ is observed at the binding energy $E_b = 31.53\,\text{eV}$ relative to E_F, the full width of peak at half maximum (FWHM) is 0.25 eV. A wide peak corresponding to the excitation of W^{4+} $4f_{5/2}$ is observed at the binding energy $E_b = 32.23\,\text{eV}$ relative to E_F, the peak FWHM is 1.2 eV. The second wide peak corresponding to the excitation of W^{6+} $4f_{5/2}$ is observed at the binding energy $E_b = 35.73\,\text{eV}$ relative to E_F, the peak FWHM is 1.40 eV. The area ratio (A) under the W $4f$ doublet core level spectrum for $A^0 : A^{4+} : A^{6+} = 2 : 3 : 5$. Figure 5, b shows a similar spectrum after gold deposition. It is shown that photoemission from the substrate is suppressed, the spectrum shape is unchanged within the measurements error. This suggests the absence of interaction between the gold atoms and substrate atoms.
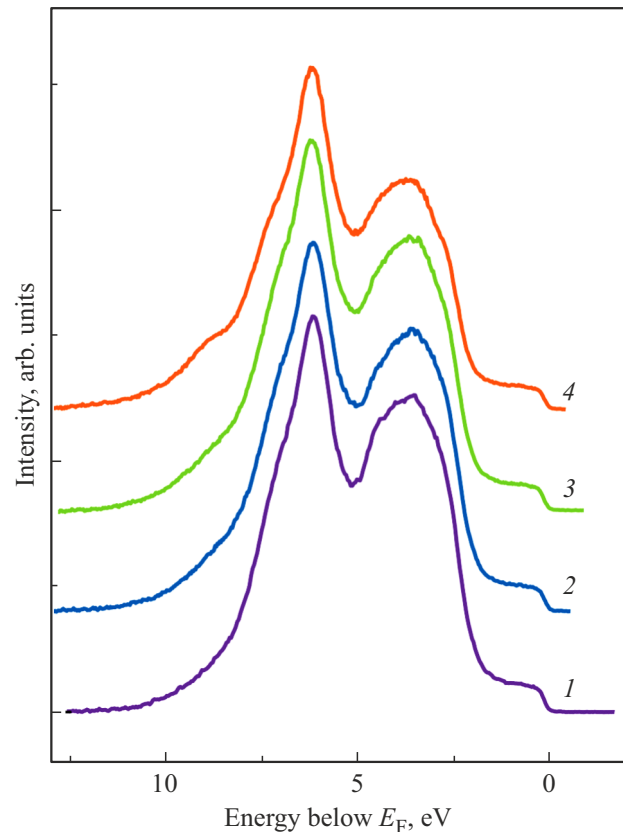
Figure 3. Normalized photoemission spectra in the VB region for the Na-Au system at the excitation energy $h\nu = 120\,\text{eV}$: *1* — clean gold surface, *2* — after deposition of 0.04 ML Na, *3* — after deposition of 0.15 ML Na, *4* — after deposition of 0.60 ML Na.

4.3. Sodium adsorption

Figures 5, c–f, 6 and 7 show the W $4f$ doublet core level spectra with the excitation energies $h\nu = 120$, 150 and $300\,\text{eV}$ after deposition of the Na submonolayer coverage. The parameters of peaks are given in Table 2. Decreasing contribution fraction of the W^{6+} states compared to the W^{4+} with the increase in the excitation energy is attributable to the fact that contribution from the states in the depth from the surface increases with the rise in excitation energy.

Deposition of the Na atom coverage equal to $\theta = 0.02\,\text{ML}$ predictably does not result in considerable changes in the W $4f$ spectrum (Figure 5, c) and slight reduction of the electron emission from the Au $4f$ core level occurs (Figure 4). A peak with a binding energy of 31.82 eV that can be attributable to the excitation of Na$^+$ states appears in the spectrum as in previous papers [4,28]. The Na$^+$ peak is not observed at $h\nu = 300\,\text{eV}$ due to a low amount of deposited Na and to the minor contribution of the surface layer compared with the emission from deeper substrate layers.

Adsorption of 0.04 ML Na atoms predictably does not result in considerable changes in the W $4f$ spectrum (Figures 5, d, 6, b and 7, b) and slight reduction of the electron
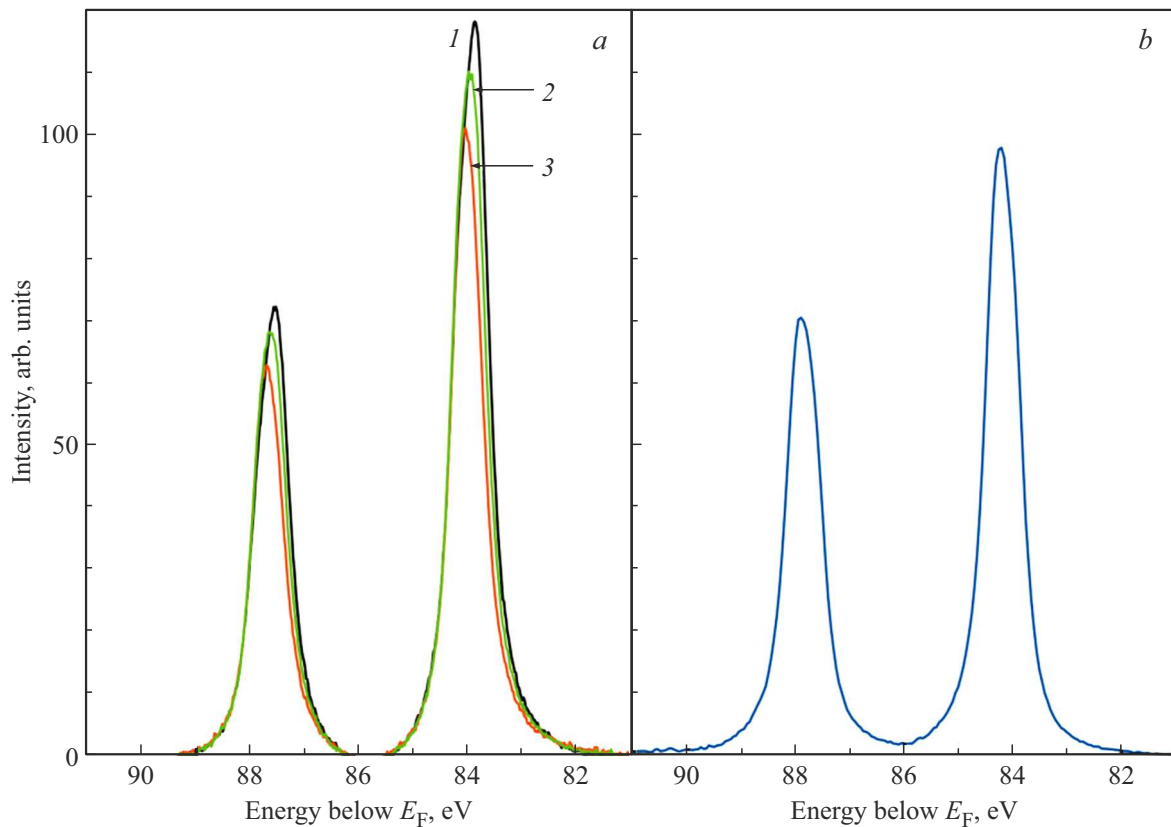
Figure 4. Normal photoemission spectra of the Au 4f (*a*) core level with the excitation energy $h\nu = 140$ eV: *1* — clean gold surface, *2* — after deposition 0.15 ML Na, *3* — after deposition 0.60 ML Na, and (*b*) for clean gold surface at the excitation energy $h\nu = 300$ eV.

Table 2. FWHM and area under the spectrum for W^0, W^{4+} and W^{6+} peaks depending on the excitation energy and coverage

$h\nu$, eV	Sodium coverage, monolayers	W		W^{4+}		W^{6+}	
		A, %	Γ, eV	A, %	Γ, eV	A, %	Γ, eV
300	0.02	21	0.26	49	1.56	30	1.70
	0.04	21	0.26	51	1.56	27	1.70
	0.15	22	0.26	51	1.60	27	1.76
	0.60	21	0.26	54	1.60	25	1.78
150	0.02	16.5	0.25	49	1.52	34	1.46
	0.04	16	0.24	51	1.52	33	1.70
	0.15	16	0.30	50	1.52	33	1.62
	0.60	15.5	0.26	54	1.8	30	1.62
120	Before Au deposition	22	0.28	30	1.2	47	1.42
	After Au deposition	18	0.25	37	1.2	45	1.46
	0.02	21	0.30	33	1.1	46	1.50
	0.04	24	0.24	37	1.2	33	1.55
	0.15	26	0.34	37	1.2	36	1.55
	0.60	25	0.35	40	1.2	34	1.55

emission from the Au 4f core level occurs (Figure 4). The adsorption of such amount of Na did not affect the W 4f spectrum shape at 300 eV unlike the W 4f spectra shown in Figures 5 and 6 at the excitation energies $h\nu = 120$ and 150 eV. Two Na peaks can be seen in the spectrum at the excitation energies $h\nu = 120$ and 150 eV. They occur at the binding energies 30.8 and 31.8 eV and may be attributable

to the excitation of the Na core levels, respectively, Na$^{\delta+}$ and Na$^+$, where δ is lower than 1. The Na$^{\delta+}$ peak position coincides with previous studies [4,28]. The wide Na$^+$ peak is attributable to the states of single Na atoms with the electron density transferred to the gold substrate and the peak width may be defined by the interaction of the absorbed Na atoms between each other with decreasing
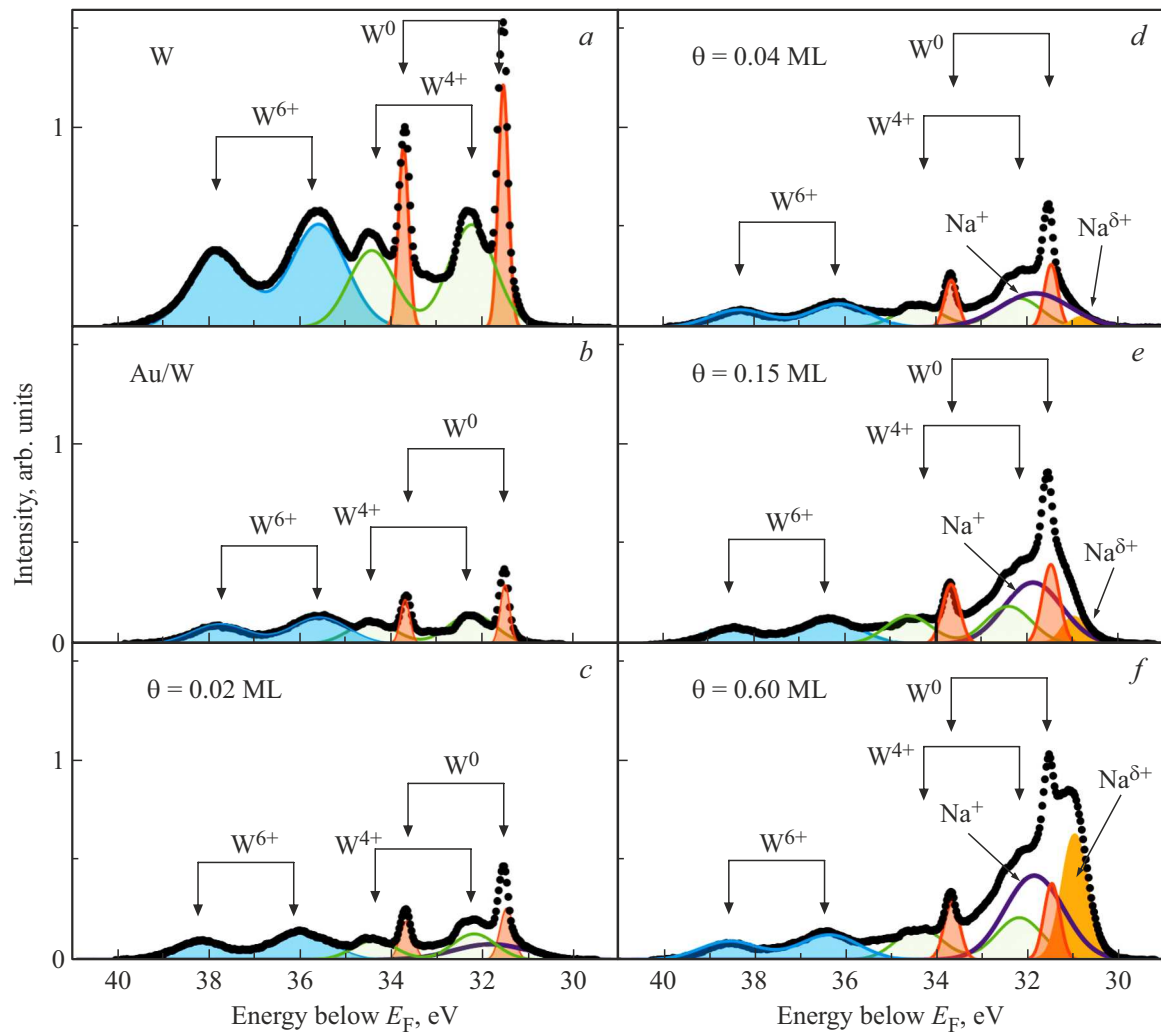
Figure 5. Photoemission spectra analysis of the W $4f$ and Na $2p$ core levels for the oxidized tungsten surface (a), after gold deposition (b) and after sodium deposition (c–f) with the excitation energy $hv = 120$ eV. Dots show the experimental spectrum, thick solid lines show contribution of W^{6+}, W^{4+}, W^0, $Na^{\delta+}$ and Na^+ states.

charge transfer to the substrate. The presence of a narrow $Na^{\delta+}$ peak with lower binding energy 30.8 eV that is close to the binding energy of 30.5 eV of Na^0 [29] suggests a lower charge state of the adsorbed Na atoms that may be explained by sufficiently strong lateral interaction of Na adatoms between each other. I.e. even at such minor Na coverage small Na islands are formed and co-exist with singe Na adatoms. The area under the Na^+ peak is 13 times larger than the area under the $Na^{\delta+}$ peak. The Na atoms adsorption has a slight effect on the parameters of the W $4f$ spectrum that is expressed only in the shift of W^{6+} peak position towards higher binding energies by 0.4 eV. It can be argued that Na atom diffusion inside the gold substrate does not occur with this coating, which agrees with the data obtained in [5]. Parameters of peaks are given in Table 3.

Adsorption of 0.15 ML Na atoms does not result in major changes in the VB spectrum (Figure 3) and only minor reduction of the electron emission from the VB takes place. Also, the Au $4f$ core level spectrum varies slightly

Table 3. Parameters of $Na^{\delta+}$ and Na^+ peaks for the Na/Au/W system depending on the excitation energy and Na coverage

hv, eV	Na, MLs	$Na^{\delta+}$			Na^+		
		A, %	E_{max}, eV	Γ, eV	A, %	E_{max}, eV	Γ, eV
150	0.02	0	—	—	100	31.61	1.40
	0.04	5	30.90	0.50	95	31.84	1.50
	0.15	13	30.94	0.50	87	31.85	1.56
	0.60	33	30.92	0.62	67	31.81	1.60
120	0.02	0	—	—	100	31.82	1.92
	0.04	7	30.83	0.46	93	31.82	1.80
	0.15	14	30.95	0.56	86	31.86	1.50
	0.60	38	30.96	0.64	62	31.86	1.52

(Figure 4) with the excitation energy of $hv = 140$ eV, with the excitation energy of $hv = 300$ eV — changes of the Au $4f$ core level spectrum are within the measurement
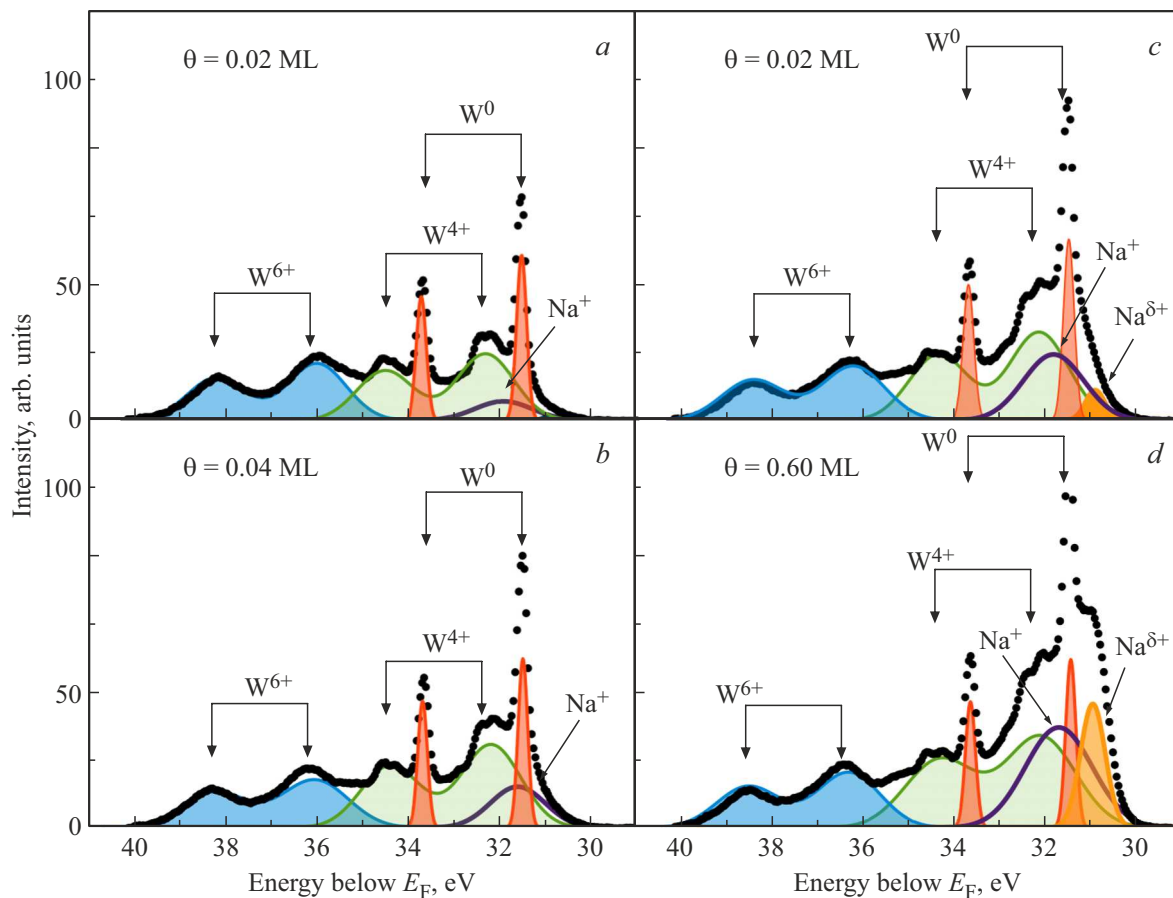
Figure 6. Photoemission spectra analysis of the W $4f$ and Na $2p$ core levels for the surface after Na deposition with the excitation energy $h\nu = 150$ eV. Dots show the experimental spectrum, thick solid lines show contribution of W^{6+}, W^{4+}, W^0, $Na^{\delta+}$ and Na^+ states.

error and therefore the spectra for this and larger Na coverage are not shown on the diagram. As shown in Figures 5, e and 7, b, Na coverage increasing from 0.04 ML to 0.15 ML did not affect the shape of W $4f$ spectra. With the excitation energy $h\nu = 300$ eV, there are no Na states in the spectrum. In the spectra obtained at the excitation energies $h\nu = 120$ and 150 eV, an increase in the area under the $Na^{\delta+}$ peak is observed compared with Na^+, and the area ratio decreases to 6. This means that Na adatom islands on the surface become larger.

Adsorption of 0.60 ML Na atoms results in considerable decrease of the photoemission intensity from the VB (Figure 3) without spectrum shape change, except for a small shoulder with the binding energy of 9.2 eV, that may be attributable to the excitation of Na states. The Au $4f$ core level spectrum also slightly changes (Figure 4, a). Figures 5−7 show that further increase of the Na dose also did not affect the W $4f$ spectrum shape. With the excitation energy $h\nu = 300$ eV, there are still no Na states in the spectrum. The tendency for an increase in the area under the $Na^{\delta+}$ peak compared to Na^+, observed with 0.15 ML sodium coverage, persists. For this coverage, the area ratio decreases to 2, demonstrating further increase of the Na adatom islands on the surface.

Na atom adsorption does not result in slight change in the VB spectrum shape (Figure 3). Emission from the VB gradually decreases with increasing deposited Na atom coverage: for $\theta = 0.15$ ML the peak with $E_b = 3.7$ eV decreases by 6%, and the peak with $E_b = 6.2$ eV decreases by 15%. A further increase of the Na coverage up to $\theta = 0.60$ ML results in a further decrease of emission from the VB: peak with $E_b = 3.7$ eV decreases by 30%, and peak with $E_b = 6.2$ eV decreases by 40%. It should be noted that a minor feature occurs at $E_b = 9.2$ eV. Drop of emission from the VB with the increase in Na coating may be attributable to the lower contribution of the Na states in the adsorbed layer compared with the contribution from the gold monolayer (see Figure 2).

The absence of tungsten oxide reduction with the deposited gold film with the thickness not higher than 2 monolayers with the Na atom adsorption confirms the non-interaction between the Na atoms and tungsten oxides. The formation of a gold film [7] according to the Vollmer-Weber mechanism is not observed, because with such gold film formation mechanism a part of the oxidized tungsten surface will be uncoated that would result in reduction of the tungsten oxides by the adsorbed Na atoms. It can be suggested that the gold film is formed on the oxidized
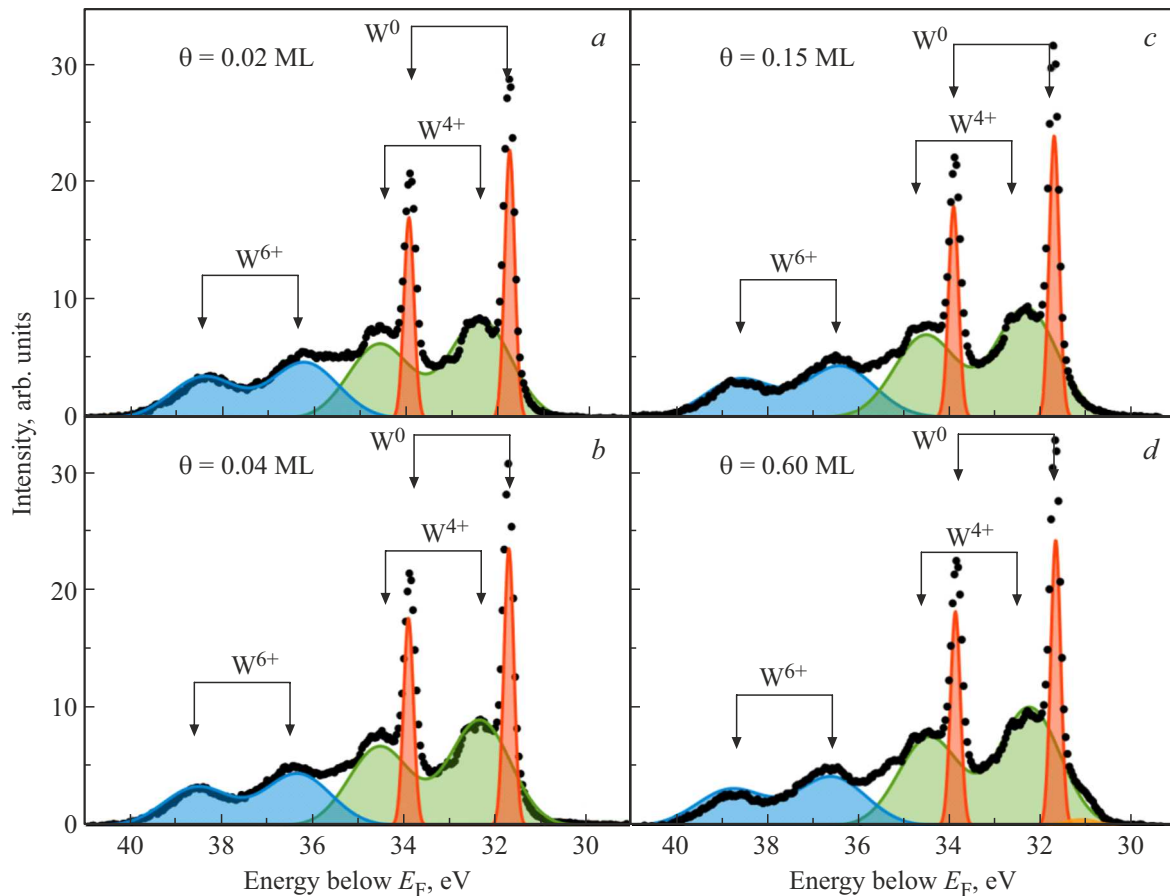
Figure 7. Photoemission spectra analysis of the W $4f$ and Na $2p$ core levels for the surface after Na deposition with the excitation energy $h\nu = 300$ eV. Dots show the experimental spectrum, thick solid lines show contribution of W^{6+}, W^{4+}, W^0, $Na^{\delta+}$ and Na^+ states.

tungsten according to the Stranski-Krastanov mechanism or the growth mechanism shown in [5,6].

5. Conclusion

It is shown that gold atom deposition on the oxidized tungsten containing two WO_3 and WO_2 oxides leads to the formation of the gold VB close to the VB of the bulk gold. The Na atom adsorption in the submonolayer range of coverages on the 2D gold film 0.83 nm thick deposited on tungsten with the surface natural oxide has been studied. The Na atom adsorption does not result in reduction of the WO_3 and WO_2 oxides that confirms the absence of Na atom diffusion inside the gold film and the layer-by-layer growth of the gold film on the oxidized tungsten, and not according to the Vollmer–Weber mechanism. Two states of the adsorbed Na atoms have been found: $Na^{\delta+}$ and Na^+. The presence of both states even with 0.60 ML Na coverage confirms that Na islands are formed during the adsorption process, besides single adsorption. The electronic structure of the 2D gold layer without and with the adsorbed Na has been calculated. It has been shown that the Na atom

adsorption is preferable in the hollow and bridge position and minor surface reconstruction occurs.

Conflict of interest

The authors declare that they have no conflict of interest.

References

[1] A. Neumann, S.L.M. Schroeder, K. Christmann. Phys. Rev. B **51**, *23*, 17007 (1995).
[2] J.V. Barth, R.J. Behm, G. Ertl. Surf. Sci. Lett. **302**, *3*, L319 (1994).
[3] J.V. Barth, R.J. Behm, G. Ertl. Surf. Sci. **341**, *1*, 62 (1995).
[4] P.A. Dement'ev, E.V. Ivanova, M.N. Lapushkin, D.A. Smirnov, S.N. Timoshnev. Phys. Solid State **62**, *8*, 1317 (2020).
[5] V.N. Ageev, E.Yu. Afanas'eva. Phys. Solid State **48**, *12*, 2347 (2006).
[6] E. Bauer, H. Poppa, G. Todd, P.R. Davis. J. Appl. Phys. **48**, *9*, 3773 (1977).
[7] E.Yu. Afanas'eva. Tech. Phys. **58**, *6*, 793 (2013).
[8] M.V. Knat'ko, V.I. Paleev, M.N. Lapushkin. Tech. Phys. **43**, *10*, 1231-1234 (1998).
[9] V.N. Ageev, Yu.A. Kuznetsov. Phys. Solid State **50**, *2*, 379 (2008).

[10] H. Shinotsuka, S. Tanuma, C.J. Powell, D.R. Penn. Surf. Interface Anal. **47**, *12*, 871 (2015).

[11] M. Klasson, J. Hedman, A. Berndtsson, R. Nilsson, C. Nordling, P. Melnik. Phys. Scr. **5**, *1−2*, 93 (1972).

[12] P. Giannozzi, S. Baroni, N. Bonini, M. Calandra, R. Car, C. Cavazzoni, D. Ceresoli, G.L. Chiarotti, M. Cococcioni, I. Dabo, A.D. Corso, S. de Gironcoli, S. Fabris, G. Fratesi, R. Gebauer, U. Gerstmann, C. Gougoussis, A. Kokalj, M. Lazzeri, L. Martin-Samos, N. Marzari, F. Mauri, R. Mazzarello, S. Paolini, A. Pasquarello, L. Paulatto, C. Sbraccia, S. Scandolo, G. Sclauzero, A.P. Seitsonen, A. Smogunov, P. Umari, R.M. Wentzcovitch. J. Phys. Condens. Matter **21**, *39*, 395502 (2009).

[13] J.P. Perdew, K. Burke, M. Ernzerhof. Phys. Rev. Lett. **77**, *18*, 3865 (1996).

[14] J.P. Perdew, J.A. Chevary, S.H. Vosko, K.A. Jackson, M.R. Pederson, D.J. Singh, C. Fiolhais. Phys. Rev. B **46**, *11*, 6671 (1992).

[15] N. Troullier, J.L. Martins. Phys. Rev. B **43**, *3*, 1993 (1991).

[16] S. Nishihara. BURAI 1.3 A GUI of Quantum ESPRESSO. https://nisihara.wixsite.com/burai (accessed 11 May 2023).

[17] V.L. Karbivskii, A.A. Romansky, L.I. Karbivska, S.I. Shulyma. Appl. Nanosci. **12**, *3*, 781 (2022). 794 p.

[18] L.-Y. Gan, Yu-Ju. Zhao. J. Chem. Phys. **133**, *9*, 094703 (2010).

[19] P.J. Goddard, J. West, R.M. Lambert. Surf. Sci. **71**, *2*, 447 (1978).

[20] S. Gurses, F. Ersan. Sci Academique **1**, *1*, 31 (2020).

[21] A. Visikovskiy, K. Mitsuhara, M. Hazama, M. Kohyama, Y. Kido. J. Chem. Phys. **139**, *14*, 144705 (2013).

[22] A. Regoutz, M. Mascheck, T. Wiell, S.K. Eriksson, C. Liljenberg, K. Tetzner, B.A.D. Williamson, D.O. Scanlon, P.l Palmgren. Rev. Sci. Instr. **89**, *7*, 073105 (2018).

[23] F.A. Stevie, C.L. Donley. J. Vac. Sci. Technol. A 38, **6**, 063204 (2020).

[24] G.H. Major, T.G. Avval, D.I. Patel, D. Shah, T. Roychowdhury, A.J. Barlow, P.J. Pigram, M. Greiner, V. Fernandez, A. Herrera-Gomez, M.R. Linford. Surf. Interface Anal. **53**, *8*, 689 (2021).

[25] S. Doniach, M. Sunjic. J. Phys. C **3**, *2*, 285 (1970).

[26] D. Cabrera-German, G. Molar-Velázquez, G. Gómez-Sosa, W. de la Cruz, A. Herrera-Gomez. Surf. Interface Anal. **49**, *11*, 1078 (2017).

[27] A.C. Simonsen, F. Yubero, S. Tougaard. Phys Rev. B **56**, *3*, 1612 (1997).

[28] A. Klein, T. Löher, C. Pettenkofer, W. Jaegermann. J. Appl. Phys. **80**, *9*, 5039 (1996).

[29] P.H. Citrin. Phys. Rev. B **8**, *12*, 5545 (1973).

Translated by E.Ilyinskaya